arXiv:nucl-th/9609047v2 11 Feb 1997

Electroproduction of the Roper resonance and the constituent quark model[a]

F. Cardarelli[(1)], E. Pace[(2)], G. Salmè[(3)], S. Simula[(3)]

[(1)] Dept. of Physics and Supercomputer Computations Research Institute
Florida State University, Tallahassee, FL 32306, USA
[(2)] Dipartimento di Fisica, Università di Roma "Tor Vergata"
and Istituto Nazionale di Fisica Nucleare, Sezione Tor Vergata
Via della Ricerca Scientifica 1, I-00133 Roma, Italy
[(3)] Istituto Nazionale di Fisica Nucleare, Sezione Sanità
Viale Regina Elena 299, I-00161 Roma, Italy

Abstract

A parameter-free evaluation of the $N - P_{11}(1440)$ electromagnetic transition form factors is performed within a light-front constituent quark model, using for the first time the eigenfunctions of a mass operator which generates a large amount of configuration mixing in baryon wave functions. A one-body electromagnetic current, which includes the phenomenological constituent quark form factors already determined from an analysis of pion and nucleon experimental data, is adopted. For Q^2 up to few $(GeV/c)^2$, at variance with the enhancement found in the elastic channel, the effect of configuration mixing results in a significant suppression of the calculated helicity amplitudes with respect to both relativistic and non-relativistic calculations, based on a simple gaussian-like ansatz for the baryon wave functions.

PACS numbers: 13.60.Rj, 13.40.Gp, 12.39.Ki, 12.39.Pn

---

[a]**To appear in Physics Letters B.**

The investigation of the electromagnetic (e.m.) excitations of nucleon resonances can shed light on their structure in terms of quarks and gluons. In this respect, the Roper resonance, $P_{11}(1440)$, plays a particular role. Within the constituent quark (CQ) picture (see, e.g., [1, 2]) this resonance is commonly assigned to a radial excitation of the nucleon, whereas it has been argued [3, 4, 5] that it might be a hybrid state, containing an explicit excited glue-field configuration (i.e., a q^3G state). Within the q^3 assignment the spin-flavour part of the Roper-resonance wave function is commonly considered to be identical to that of the nucleon, whereas the q^3G state is directly orthogonal to the nucleon in the spin-flavour space. Then, it is expected [4] that such different spin structures of the Roper resonance could lead to different behaviours of its e.m. helicity amplitudes as a function of the four-momentum transfer, so that future experiments planned at $TJNAF$ [6] might provide signatures for hybrid baryons. However, the predictions of Ref. [4] have been obtained within a non-relativistic framework and using simple gaussian-like wave functions. Within the CQ model, the relevance of the relativistic effects on the helicity amplitudes of the Roper resonance has been illustrated by Weber [7] and by Capstick and Keister [2], where (we stress) gaussian-like wave functions were still adopted.

The purpose of this letter is to compute the e.m. $N - P_{11}(1440)$ transition form factors in the relativistic CQ model developed in [8, 9, 10]. The model incorporates the following features: i) a proper treatment of relativistic effects through the light-front (LF) formalism; ii) the use of the eigenfunctions of a baryon mass operator having a much closer connection to the mass spectrum with respect to a gaussian-like ansatz; iii) the use of a one-body approximation for the e.m. current able to reproduce the experimental data on the nucleon form factors. Inside baryons the CQ's are assumed to interact via the $q - q$ potential of Capstick and Isgur (CI) [11]. A relevant feature of this interaction is the presence of an effective one-gluon-exchange (OGE) term, which produces a huge amount of high-momentum components and $SU(6)$ breaking terms in the baryon wave functions (see [9, 10]); in what follows we will refer to these effects as the configuration mixing. Finally, an effective one-body e.m. current, including Dirac and Pauli form factors for the CQ's (cf. also Ref. [12]), is adopted. The CQ form factors have been determined in [9] using as constraints the pion and nucleon experimental data. In [10] our parameter-free prediction for the magnetic form factor of the $N - \Delta(1232)$ transition has been checked against available data. In this letter, our parameter-free results for the $N - P_{11}(1440)$ helicity amplitudes will be presented, showing that the configuration mixing leads to a significant suppression of the calculated helicity amplitudes with respect to relativistic as well as non-relativistic calculations, based on a simple gaussian-like ansatz for the wave functions.

In the LF hamiltonian dynamics (cf. [13]) intrinsic momenta of the CQ's, k_i, can be obtained from the on-mass-shell momenta p_i in a general reference frame, through the LF boost $L_f^{-1}(P_0)$, which transforms the momentum $P_0 \equiv \sum_{i=1}^3 p_i$ as $L_f^{-1}(P_0) \, P_0 = (M_0, 0, 0, 0)$ without Wigner rotations. Thus, one has $k_i = L_f^{-1}(P_0) \, p_i$ and, obviously, $\sum_{i=1}^3 \vec{k}_i = 0$. In this formalism a baryon state in the $u - d$ sector, $|\Psi_{JJ_n \ \pi}^{TT_3}, \tilde{P}\rangle$, is an eigenstate of: i) isospin, T and T_3; ii) parity, π; iii) kinematical (non-interacting) LF angular momentum operators j^2 and j_n, where the vector $\hat{n} = (0, 0, 1)$ defines the spin quantization axis; iv) total LF

baryon momentum $\tilde{P} \equiv (P^+, \vec{P}_\perp) = \tilde{p}_1 + \tilde{p}_2 + \tilde{p}_3$, where $P^+ = P^0 + \hat{n} \cdot \vec{P}$ and $\vec{P}_\perp \cdot \hat{n} = 0$. We explicitly construct $|\Psi^{TT_3}_{JJ_n \pi}, \tilde{P}\rangle$ as eigenstate of an intrinsic LF mass operator, $\mathcal{M} = M_0 + \mathcal{V}$, where $M_0 = \sum_{i=1}^3 \sqrt{m_i^2 + \vec{k}_i^2}$ is the free mass operator, m_i the CQ mass and $\mathcal{V}$ a Poincaré invariant interaction. The state $|\Psi^{TT_3}_{JJ_n \pi}, \tilde{P}\rangle$ factorizes into $|\Psi^{TT_3}_{JJ_n \pi}\rangle |\tilde{P}\rangle$ and the intrinsic LF angular momentum eigenstate $|\Psi^{TT_3}_{JJ_n \pi}\rangle$ can be constructed from the eigenstate $|\psi^{TT_3}_{JJ_n \pi}\rangle$ of the *canonical* angular momentum, i.e. $|\Psi^{TT_3}_{JJ_n \pi}\rangle = \mathcal{R}^\dagger |\psi^{TT_3}_{JJ_n \pi}\rangle$, by means of the unitary operator $\mathcal{R}^\dagger = \prod_{j=1}^3 R^\dagger_{Mel}(\vec{k}_j, m_j)$, with $R_{Mel}(\vec{k}_j, m_j)$ being the generalized Melosh rotation [13]. One gets

$$(M_0 + V) \, |\psi^{TT_3}_{JJ_n \pi}\rangle \;=\; M \, |\psi^{TT_3}_{JJ_n \pi}\rangle \tag{1}$$

where M is the baryon mass. The interaction $V = \mathcal{R}\mathcal{V}\mathcal{R}^\dagger$ has to be independent of the total momentum P and invariant upon spatial rotations and translations (cf. [13]). We can identify Eq. (1) with the baryon mass equation proposed by Capstick and Isgur in [11]. The CI effective interaction $V = \sum_{i<j} V_{ij}$ is composed by a linear confining term (dominant at large separations) and a OGE term (dominant at short separations). The latter contains both a central Coulomb-like potential and a spin-dependent part, responsible for the hyperfine splitting of baryon masses. The values $m_u = m_d = 0.220 \; GeV$ [11] have been adopted throughout this work. As in Refs. [9, 10], the mass equation (1) has been solved by expanding the state $|\psi^{TT_3}_{JJ_n \pi}\rangle$ onto a (truncated) set of harmonic oscillator (HO) basis states and by applying the Rayleigh-Ritz variational principle. We have included in the expansion all the HO basis states up to 20 HO quanta and the obtained eigenvalues are in agreement with the results of Ref. [11]. The S, S' and D components have been considered and the corresponding probabilities are: $P_S^N = 98.1\%$, $P_{S'}^N = 1.7\%$, $P_D^N = 0.2\%$ for the nucleon and $P_S^{Roper} = 90.6\%$, $P_{S'}^{Roper} = 9.3\%$, $P_D^{Roper} = 0.1\%$ for the Roper resonance. Note that in [14] an approximate treatment of the hyperfine OGE term led to: $P_S^{Roper} \simeq 97\%$, $P_{S'}^{Roper} \simeq 3\%$, $P_D^{Roper} \simeq 0.01\%$. Finally, P partial waves have been neglected, because they do not couple to the main components of the wave functions.

Let us now consider the CQ momentum distribution $n(p)$, defined as in [10]. The momentum distribution $n(p)$, times p^2, obtained for the nucleon and the Roper resonance using the CI interaction, is shown in Fig. 1(a) and compared with the gaussian-like ansatz adopted in [2]. It can clearly be seen that the high-momentum tail of both baryon wave functions is sharply enhanced by the effects due to the OGE interaction. The contributions of the S, S' and D partial waves to the CQ momentum distribution are separately shown in Fig. 1(b). It turns out that in case of the Roper resonance the mixed-symmetry S'-wave, which has a spin-flavour structure orthogonal to that of the symmetric S-wave component, yields a significant contribution in a wide range of momenta; moreover, for $p \lesssim 1 \; GeV/c$ the S' component is much larger in the Roper resonance than in the nucleon. On the contrary, the D-wave components of both the nucleon and the Roper resonance give a negligible contribution to $n(p)$. Therefore, in the calculation of the $N - P_{11}(1440)$ transition form factors we will neglect the contribution of D-wave components. The results reported in Fig. 1 clearly show that, when the OGE interaction is fully considered, the resulting CQ

structure of the Roper resonance contains high radial excitations and sizable mixed-symmetry components, so that it can hardly be interpreted as a simple (first) radial excitation of the nucleon.

The matrix elements of the e.m. $N - P_{11}(1440)$ transition current can be written as follows (cf., e.g., [7])

$$\langle\Psi^{\frac{1}{2}\tau^*}_{\frac{1}{2}\nu^*\ +1}, \tilde{P}^*|\ \mathcal{I}^\mu(0)\ |\Psi^{\frac{1}{2}\tau}_{\frac{1}{2}\nu\ +1}, \tilde{P}\rangle = \delta_{\tau^*\tau}\ \mathcal{I}^\mu_{\nu^*\nu}(\tau) =$$

$$\delta_{\tau^*\tau}\ \bar{u}(\tilde{P}^*, \nu^*)\left\{F_1^{*\tau}(Q^2)\ [\gamma^\mu + q^\mu\frac{M^* - M}{Q^2}] + F_2^{*\tau}(Q^2)\ \frac{i\sigma^{\mu\rho}q_\rho}{M^* + M}\right\}u(\tilde{P}, \nu) \qquad (2)$$

where $Q^2 \equiv -q\cdot q$ is the squared four-momentum transfer, $\sigma^{\mu\rho} = \frac{i}{2}[\gamma^\mu, \gamma^\rho]$, $u(\tilde{P}, \nu)$ $[u(\tilde{P}^*, \nu^*)]$ the nucleon [Roper-resonance] spinor, $F_{1(2)}^{*\tau}(Q^2)$ the Dirac (Pauli) form factor associated to the $N - P_{11}(1440)$ transition and $\tau = \mp1/2$ (or $\tau = n, p$). In Eq. (2) the structure $\gamma^\nu + q^\mu(M^* - M)/Q^2$ is required in order to keep gauge invariance. In the LF formalism (cf. [13]) the space-like e.m. form factors are related to the matrix elements of the *plus* component of the e.m. current ($\mathcal{I}^+$) and, moreover, the choice $q^+ = P^{*+} - P^+ = 0$ allows to suppress the contribution of the pair creation from the vacuum [15]. The matrix elements $\mathcal{I}^+_{\nu^*\nu}(\tau)$ can be cast in the form $\mathcal{I}^+_{\nu^*\nu}(\tau) = F_1^{*\tau}(Q^2)\delta_{\nu^*\nu} - F_2^{*\tau}(Q^2)\ i(\sigma_2)_{\nu^*\nu}\ Q/(M^*+M)$, where σ_2 is a Pauli matrix. Then, the transition form factors $F_{1(2)}^{*\tau}(Q^2)$ are given by $F_1^{*\tau}(Q^2) = Tr[\mathcal{I}^+(\tau)]/2$ and $F_2^{*\tau}(Q^2) = i(M^* + M)\ Tr[\sigma_2\ \mathcal{I}^+(\tau)]/2Q$.

The $N - P_{11}(1440)$ transition form factors will be evaluated using the eigenvectors of Eq. (1) and the plus component of the one-body e.m. current of Ref. [9], viz.

$$\mathcal{I}^+(0) = \sum_{j=1}^3 I_j^+(0) = \sum_{j=1}^3 \left(e_j\gamma^+ f_1^j(Q^2)\ +\ i\kappa_j\frac{\sigma^{+\rho}q_\rho}{2m_j}f_2^j(Q^2)\right) \qquad (3)$$

where e_j (κ_j) is the charge (anomalous magnetic moment) of the j-th quark, and $f_{1(2)}^j$ its Dirac (Pauli) form factor. Though the full hadron e.m. current has to include two-body components for fulfilling gauge and rotational invariances (see [13]), we have shown [9] that the effective one-body current component (3) is able to give a coherent description of both the pion and nucleon experimental form factors. Moreover, using the CQ form factors determined in [9], our parameter-free prediction for the magnetic form factor of the $N - \Delta(1232)$ transition has been checked against available data (see [10]). Let us stress that, since our one-body approximation refers to the $\mathcal{I}^+$ component of the current only, with a suitable definition of the other components the e.m. current can fulfil gauge invariance.

Our results for the magnetic transition form factor $G_M^{*p}(Q^2) \equiv F_1^{*p}(Q^2) + F_2^{*p}(Q^2)$, obtained using the CI wave functions both with and without the CQ form factors of Refs. [9, 10], are shown in Fig. 2 for Q^2 up to few $(GeV/c)^2$ (i.e., in a range of values of Q^2 of interest to $TJNAF$) and compared with the predictions of the relativistic q^3 model of Ref. [2], where a gaussian-like ansatz is adopted for the baryon wave functions and point-like CQ's are assumed. As in the case of the elastic $G_M^p(Q^2)$ form factor (cf. Ref. [9]), $G_M^{*p}(Q^2)$ is remarkably sensitive to configuration mixing effects. However, for Q^2 up to few $(GeV/c)^2$ it

4

turns out that the configuration mixing does not produce in $G_M^{*p}(Q^2)$ the large enhancement found in the elastic channel. Then, when the CQ form factor of Ref. [9] are included, our full prediction and the one of Ref. [2] turn out to be quite similar for the proton, but strongly different for the $p - P_{11}(1440)$ transition. In particular, for $Q^2 \sim 1 \div 4$ $(GeV/c)^2$ our magnetic form factor $G_M^{*p}(Q^2)$ is suppressed with respect to the prediction of Ref. [2] by a large factor $(\sim 3 \div 4)$, which implies a reduction of about one order of magnitude for the electroproduction cross section of the Roper resonance.

In what follows, our results will be shown in terms of the helicity amplitudes $A_{\frac{1}{2}}^{\tau}(Q^2)$ and $S_{\frac{1}{2}}^{\tau}(Q^2)$, defined as

$$A_{\frac{1}{2}}^{\tau}(Q^2) = \mathcal{N}(Q^2)\, G_M^{*\tau}(Q^2) \quad , \quad S_{\frac{1}{2}}^{\tau}(Q^2) \;=\; \mathcal{N}(Q^2)\frac{\sqrt{2K^-K^+}}{Q^2}\frac{M^*+M}{4M^*}\, G_E^{*\tau}(Q^2) \quad (4)$$

where $\mathcal{N} \equiv \sqrt{\frac{\pi\alpha}{K^*}\frac{K^-}{M^*M}}$, $K^{\pm} \equiv Q^2 + (M^* \pm M)^2$, $K^* \equiv (M^{*2} - M^2)/2M^*$ and $G_E^{*\tau} \equiv F_1^{*\tau} - Q^2\, F_2^{*\tau}/(M^* + M)^2$. Our parameter-free predictions for $A_{\frac{1}{2}}^{p(n)}(Q^2)$ and $-S_{\frac{1}{2}}^{p(n)}(Q^2)$ are shown in Fig. 3 and compared with the photoproduction values [16] and the results of phenomenological analyses [17, 18] of available electroproduction data, as well as with the predictions of the relativistic q^3 model of Ref. [2] and of the non-relativistic q^3 and q^3G models of Ref. [4](c). Moreover, in order to better illustrate the effects of the configuration mixing, the result obtained excluding the S' component of the CI wave functions of both the nucleon and the Roper resonance, is also reported in Fig. 3. As in case of $G_M^{*p}(Q^2)$, our results both for the transverse $A_{\frac{1}{2}}^{p(n)}(Q^2)$ and the longitudinal $S_{\frac{1}{2}}^p(Q^2)$ helicity amplitudes exhibit a remarkable reduction with respect to non-relativistic as well as relativistic predictions, based on simple gaussian-like wave functions. Such a reduction brings our predictions closer to the results of the phenomenological analyses of Refs. [17, 18][b]. At the photon point it can be seen that: i) our prediction for $A_{\frac{1}{2}}^n(Q^2 = 0)$ agrees well with the PDG value [16], while the absolute value of $A_{\frac{1}{2}}^p(Q^2 = 0)$ is underestimated; ii) the longitudinal helicity amplitudes $S_{\frac{1}{2}}^p(Q^2 = 0)$ and $S_{\frac{1}{2}}^n(Q^2 = 0)$ are remarkably sensitive to the presence of the mixed-symmetry S' component in the CI wave functions. The latter feature holds as well up to $Q^2 \sim$ few $(GeV/c)^2$, whereas the transverse helicity amplitudes $A_{\frac{1}{2}}^{p(n)}(Q^2)$ are only slightly modified by the S' partial waves. Finally, it turns out that the relativistic predictions of the ratio $A_{\frac{1}{2}}^n(Q^2)/A_{\frac{1}{2}}^p(Q^2)$ differ remarkably from the non-relativistic result of the q^3 and q^3G models (i.e., $A_{\frac{1}{2}}^n(Q^2)/A_{\frac{1}{2}}^p(Q^2) = -2/3$). This result, which is clearly crucial in a comparison with experimental data, is mainly due to S' components and to kinematical relativistic effects associated to the Melosh rotations; in particular, at the photon point we obtain: $A_{\frac{1}{2}}^n/A_{\frac{1}{2}}^p \simeq -4/3$ and $\simeq -1.1$ with and without the S' components, respectively.

Recently [4](c), it has been argued that the uncertainties related to the lack of a precise knowledge of the baryon wave functions might cancel out in the ratio between transverse and

---

[b]It should be reminded that model-dependent assumptions made in Refs. [17, 18] might produce significant uncertainties in the data analyses.

longitudinal helicity amplitudes. Thus, in order to check this point, our predictions for the ratio $A_{\frac{1}{2}}^p(Q^2)/[-S_{\frac{1}{2}}^p(Q^2)]$ are shown in Fig. 4 and compared with the results of non-relativistic [4](c) and relativistic [2] calculations, based on a simple gaussian-like ansatz for the baryon wave functions. It can clearly be seen that up to $Q^2 \sim 2$ $(GeV/c)^2$ the ratio exhibits a small sensitivity to configuration mixing effects as well as to the e.m. structure of the CQ's, whereas it is strongly modified by relativistic effects. In this respect we want to stress that the relevance of the effects due to the relativistic compositions of the CQ spins, firstly shown in [7] and clearly exhibited in Figs. 3 and 4, suggests that these effects, as well as those arising from the configuration mixing, should be fully included in the predictions of the hybrid q^3G model, before a meaningful comparison with our light-front CQ picture can be performed. Finally, note that for $Q^2 \sim 0.2 \div 0.6$ $(GeV/c)^2$ the relativistic predictions of the transverse amplitudes change sign, independently of the effects from the configuration mixing and the CQ form factors; therefore, for $Q^2 \sim 0.2 \div 0.6$ $(GeV/c)^2$ the Roper-resonance production cross section is expected to be mainly governed by its longitudinal helicity amplitude.

In conclusion, the $N - P_{11}(1440)$ electromagnetic transition form factors have been analyzed within a light-front constituent quark model, using for the first time baryon wave functions, which incorporate the configuration mixing generated by the effective one-gluon-exchange potential of Ref. [11], and a one-body electromagnetic current, which includes the phenomenological constituent quark form factors determined in [9] from an analysis of pion and nucleon experimental data. It has been shown that the effects of the configuration mixing (i.e., high-momentum components and $SU(6)$ breaking terms) in the Roper-resonance wave function are large and prevent to consider the structure of this resonance as a simple (first) radial excitation of the nucleon. It has been found that the configuration mixing yields a remarkable suppression of the calculated helicity amplitudes with respect to relativistic and non-relativistic predictions, based on a simple gaussian-like ansatz for the baryon wave functions. Moreover, the longitudinal helicity amplitudes exhibit an appreciable sensitivity to the mixed-symmetry S' components, generated in the baryon wave functions by the hyperfine interaction.

References

[1] R. Koniuk and N. Isgur: Phys. Rev. **D21** (1980) 1868.

[2] S. Capstick and B. Keister: Phys. Rev. **D 51** (1995) 3598.

[3] T. Barnes and F.E. Close: Phys. Lett. **B123** (1983) 89; *ib.* **B128** (1983) 277.

[4] (a) Z. Li and F.E. Close: Phys. Rev. **D42** (1990) 2207. (b) Z. Li: Phys. Rev. **D44** (1991) 2841. (c) Z. Li, V. Burkert and Z. Li: Phys. Rev. **D46** (1992) 70.

[5] C.E. Carlson and N.C. Mukhopadhyay: Phys. Rev. Lett. **67** (1991) 3745.

[6] TJNAF proposals: 89-038, spokespersons V.D. Burkert, M. Gai and R. Minehart; 91-002, spokespersons P. Stoler, V.D. Burkert and M. Taiuti; 93-036, spokespersons R. Chasteler, R. Minehart and H. Weller. See, also, V.D. Burkert: AIP Conf. Proc. **334** (1995) 127, ed. by F. Gross.

[7] H.J. Weber: Phys. Rev. **C41** (1990) 2783.

[8] F. Cardarelli et al.: Phys. Lett. **332B** (1994) 1; Phys. Rev. **D53** (1996) 6682; Phys. Lett. **B349** (1995) 393; Phys. Lett. **B359** (1995) 1; Few-Body Syst. Suppl. **9** (1995) 267.

[9] F. Cardarelli, E. Pace, G. Salmè and S. Simula: Phys. Lett. **B357** (1995) 267; Few-Body Syst. Suppl. **8** (1995) 345.

[10] F. Cardarelli, E. Pace, G. Salmè and S. Simula: Phys. Lett. **B371** (1996) 7.

[11] S. Capstick and N. Isgur, Phys. Rev. **D 34** (1986) 2809.

[12] S. Foster and G. Hughes, Z. Phys. **C14** (1982) 123; Rep. Prog. Theor. Phys. **46** (1983) 1445.

[13] B.D. Keister and W.N. Polyzou, Adv. in Nucl. Phys. **20** (1991) 225. F. Coester, Prog. in Part. and Nucl. Phys. **29** (1992) 1.

[14] N. Isgur and G. Karl: Phys. Rev. **D19** (1979) 2653.

[15] L. Frankfurt and M. Strikman, Nucl. Phys. **B 148** (1979) 107. G.P. Lepage and S.J. Brodsky, Phys. Rev. **D 22** (1980) 2157.

[16] Particle Data Group, R.M. Barnett et al.: Phys. Rev. **D54** (1996) 1.

[17] C. Gerhardt: Z. Phys. **C4** (1980) 311.

[18] B. Boden and G. Krosen: in Proc. of the Conf. on *Research Program at CEBAF II*, ed. by V. Burkert et al., CEBAF (USA), 1986.

Figure Captions

Fig. 1. (a) The momentum distribution $n(p)$ of the constituent quarks in the nucleon (thick lines) and in the Roper resonance (thin lines), times p^2. The solid and dashed lines are the CQ momentum distributions obtained from the eigenstates of Eq. (1) with the CI interaction [11] and those corresponding to the gaussian-like ansatz, adopted in [2], respectively. (b) Contributions of various partial waves to the CQ momentum distribution (times p^2) in the nucleon (thick lines) and in the Roper resonance (thin lines), obtained using the CI interaction. The solid, dashed and dot-dashed lines correspond to the S, S' and D partial-wave contributions, respectively.

Fig. 2. The magnetic form factor $G_M^{*p}(Q^2)$ for the $p - P_{11}(1440)$ transition versus Q^2. The solid line is our prediction, obtained using the eigenstates of the mass equation (1) with the CI interaction and the one-body current component (3) with the CQ form factors of Ref. [9]. The dotted line is obtained with the CI wave functions, but assuming point-like CQ's (i.e., putting in Eq. (3) $f_1^j = 1$ and $\kappa_j = 0$). The dot-dashed line is the result of Ref. [2], obtained using a simple gaussian-like ansatz for the baryon wave functions and assuming point-like CQ's.

Fig. 3. The $N - P_{11}(1440)$ helicity amplitudes $A_{\frac{1}{2}}^{p(n)}(Q^2)$ and $-S_{\frac{1}{2}}^{p(n)}(Q^2)$, as a function of Q^2. The full dots are the PDG values [16], while the full squares and open dots are the results of the analysis of available electroproduction data performed in Refs. [17] and [18], respectively. Thick lines correspond to the results of LF calculations. The solid and dot-dashed lines are the same as in Fig. 2. The dashed lines are the results of our calculations performed excluding the S'-wave components of the CI wave functions of both the nucleon and the Roper resonance. Thin lines are the results of non-relativistic calculations of Ref. [4](c). The long-dashed and dot-dashed lines correspond to the q^3G and q^3 models, evaluated using Eqs. (5) and (8) of Ref. [4](c), respectively. Note that within the hybrid q^3G model $S_{\frac{1}{2}}^{p(n)}(Q^2) = 0$, whereas only $S_{\frac{1}{2}}^n(Q^2)$ is vanishing within the non-relativistic q^3 model. In (b) and (d) the error bars on the solid thick line represent the uncertainties related to the numerical Monte Carlo integration procedure.

Fig. 4. Ratio of the transverse $A_{\frac{1}{2}}^p(Q^2)$ to the longitudinal $-S_{\frac{1}{2}}^p(Q^2)$ helicity amplitudes of the $p - P_{11}(1440)$ transition, as a function of Q^2. Thick lines correspond to the results of LF calculations. The solid, dashed, dotted and dot-dashed lines are the same as in Figs. 2 and 3. The thin dot-dashed line is the prediction of the non-relativistic q^3 model of Ref. [4](c). The erros bars are as in Fig. 3.
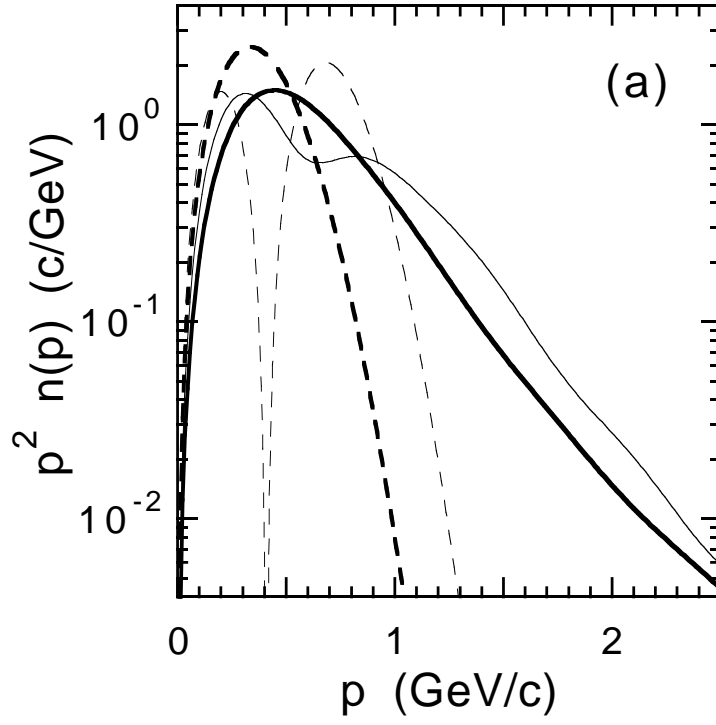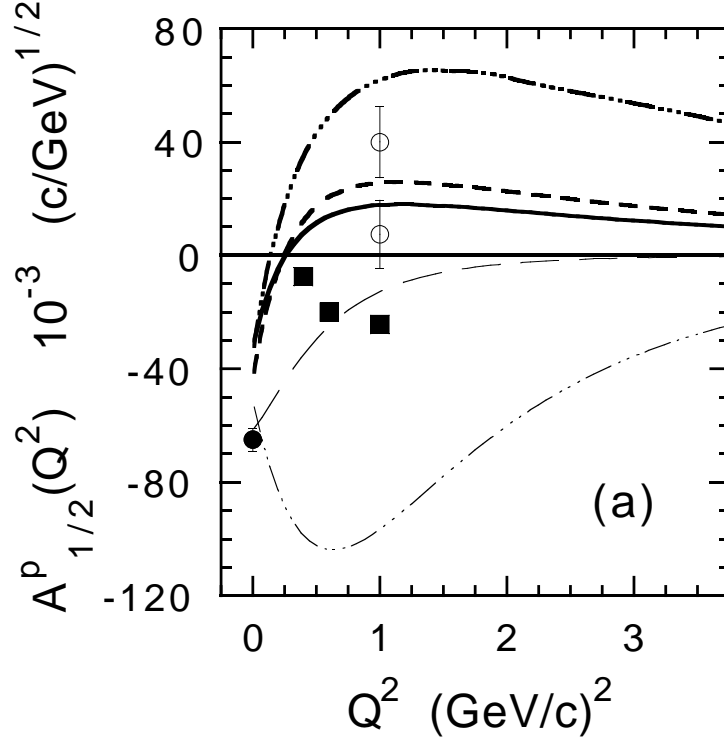
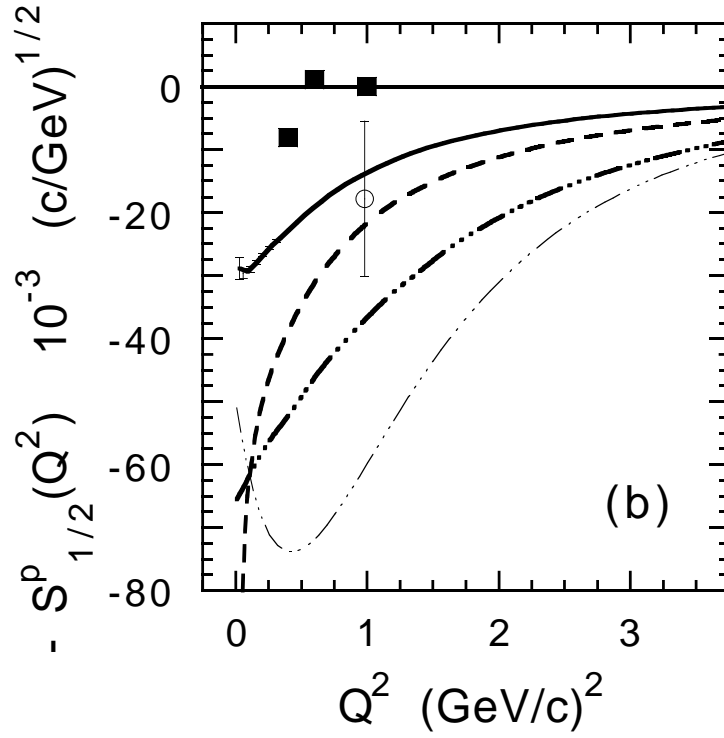F. Cardarelli, E. Pace, G. Salmè, S. Simula, Phys. Lett. B: fig. 1a
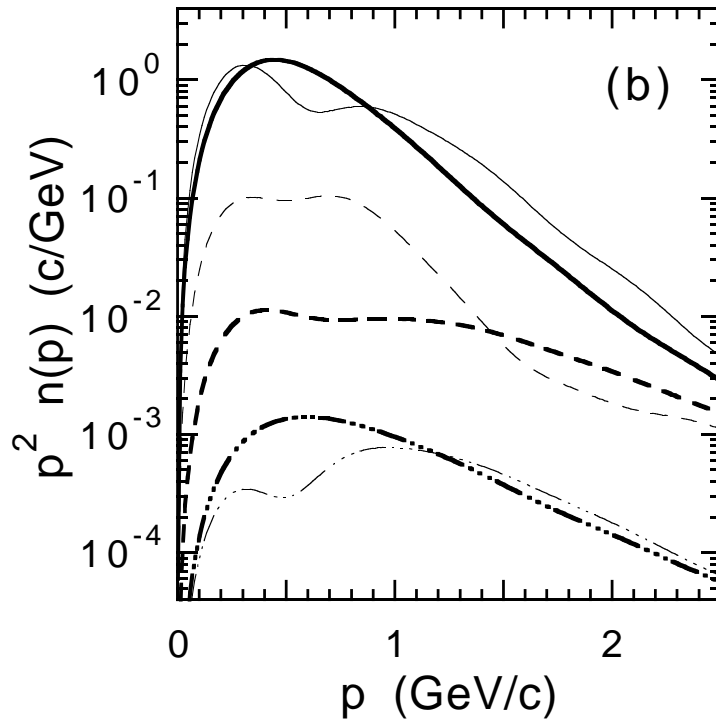
F. Cardarelli, E. Pace, G. Salmè, S. Simula, Phys. Lett. B: fig. 1b
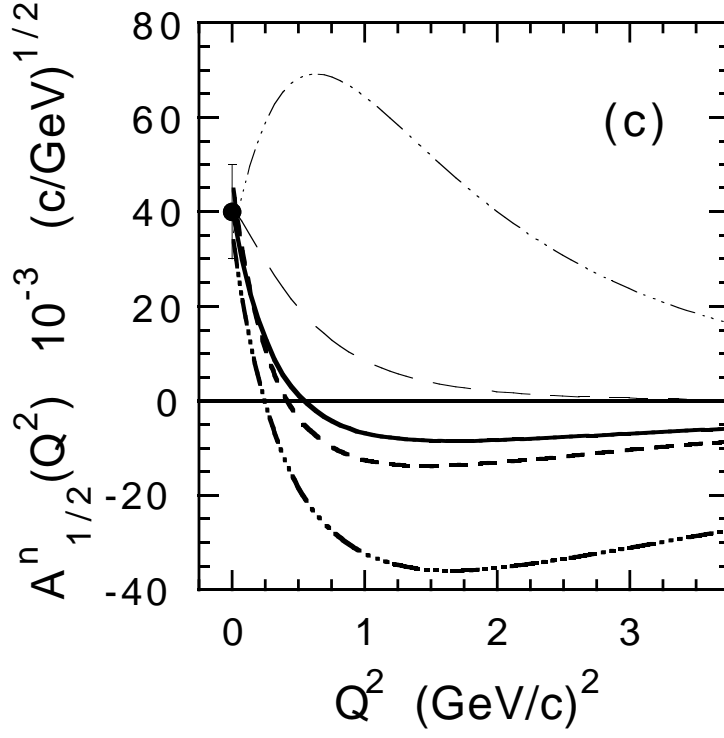
9
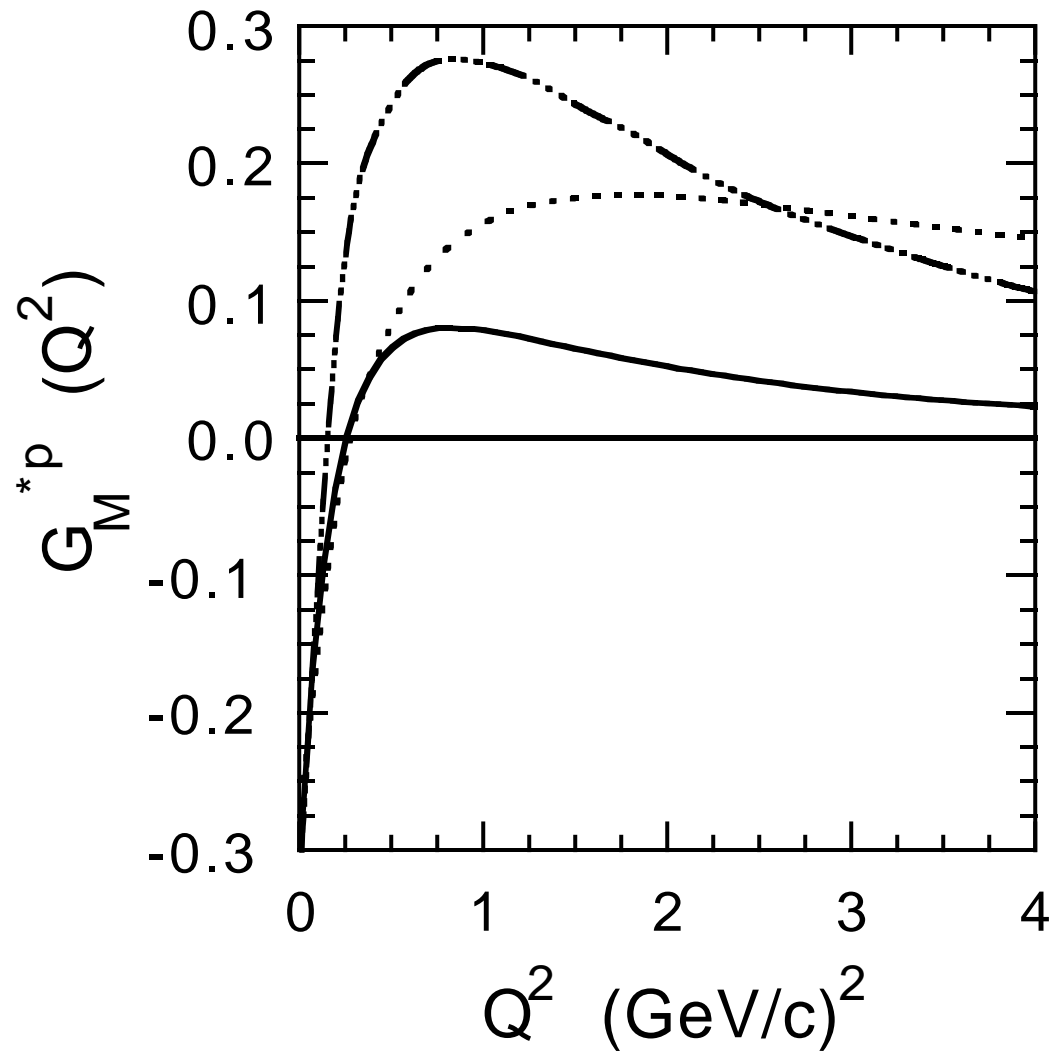
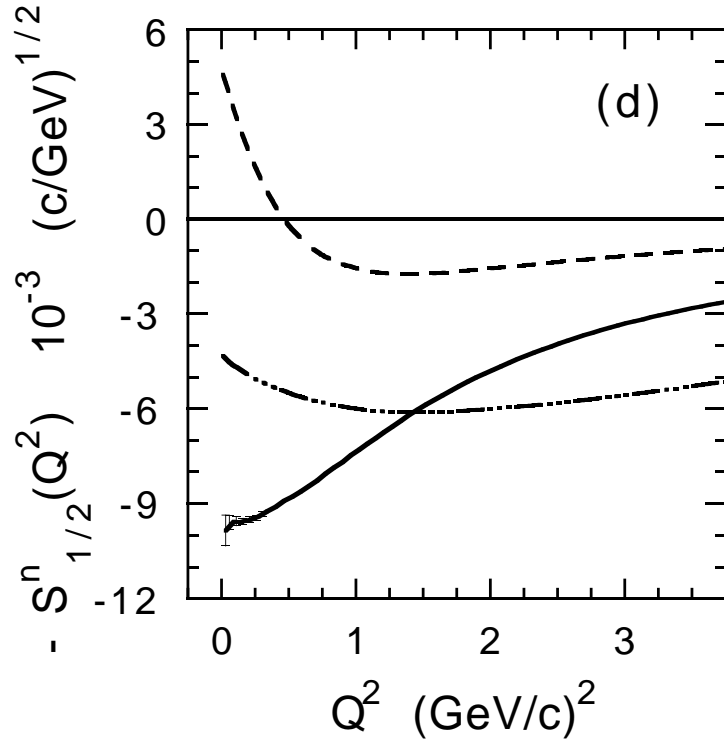F. Cardarelli, E. Pace, G. Salmè, S. Simula, Phys. Lett. B: fig. 2

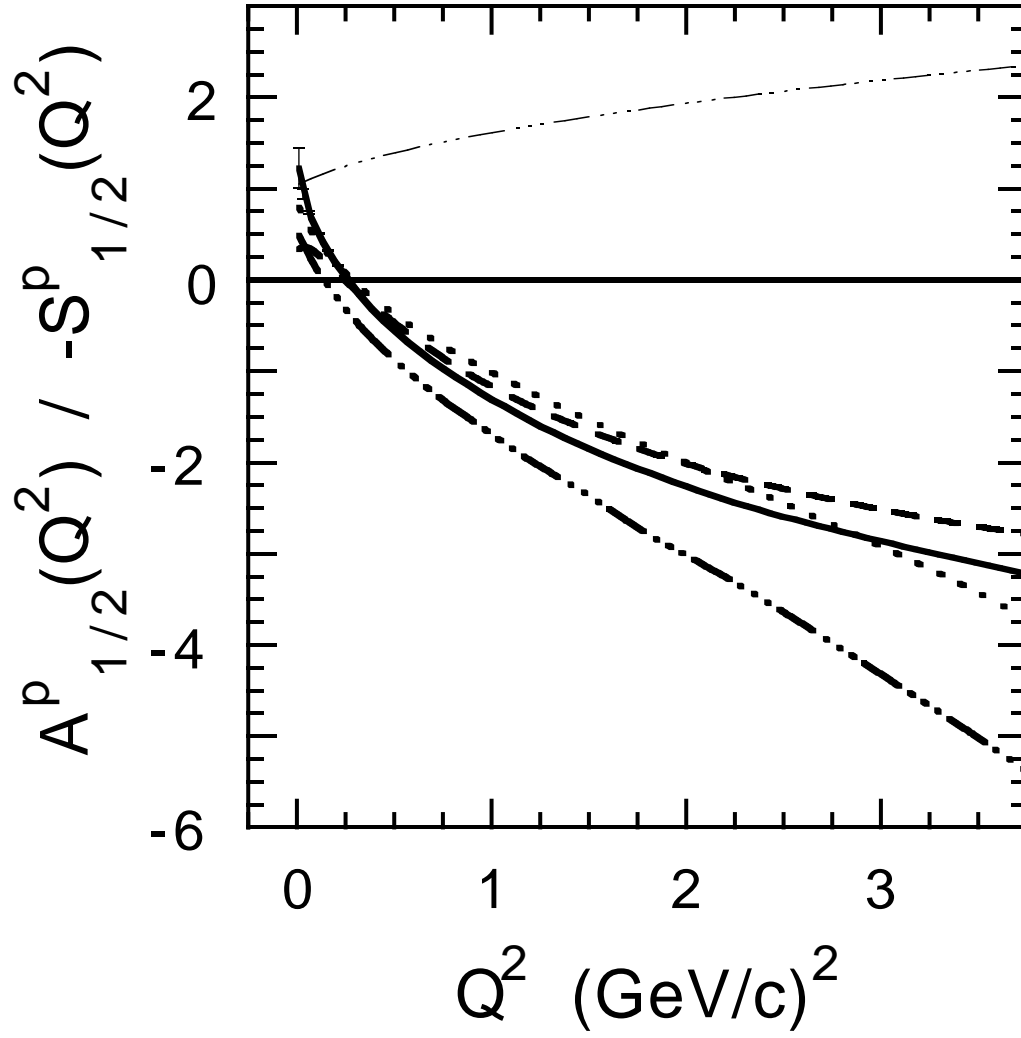F. Cardarelli, E. Pace, G. Salmè, S. Simula, Phys. Lett. B: fig. 3a

F. Cardarelli, E. Pace, G. Salmè, S. Simula, Phys. Lett. B: fig. 3b

F. Cardarelli, E. Pace, G. Salmè, S. Simula, Phys. Lett. B: fig. 3c

F. Cardarelli, E. Pace, G. Salmè, S. Simula, Phys. Lett. B: fig. 3d

12

F. Cardarelli, E. Pace, G. Salmè, S. Simula, Phys. Lett. B: fig. 4